

Composite bond inspection

Robert Lee Crane · Giles Dillingham

Received: 7 April 2008 / Accepted: 30 April 2008 / Published online: 13 August 2008
© Springer Science+Business Media, LLC 2008

Abstract After 50+ years of research to discover a way of determining the in situ strength of an adhesive bond, a method has been found to probe this key parameter. The initial testing on composite joints has shown it to be accurate and reliable. While effective, it is expensive to implement in a production environment and then during the final stages of assembly. A second method of probing the adherent surface prior to bonding is presented that offers the promise of determining adhesion potential before final bond consolidation. These new inspection methods should enable significant increases in structural performance for structures that utilize composite materials. Before examining these two new methods a brief review of past work on adhesive bond strength determination is presented.

Introduction

Composite materials are chiefly used for secondary aircraft components while primary structural components are fabricated from traditional metals. A major impediment to the wider application of composites in aerospace structures has been the lack of a reliable and efficient joining method. Metallic structures, on the other hand, are assembled from subcomponents to produce larger structures via mechanical fastening or metallurgical bonding, e.g., welding, brazing,

diffusion bonding, etc. Unfortunately, mechanical fastening does not allow the aircraft designer to utilize the many structural advantages of composites. Adhesive bonding would be the preferred joining method for composites, but is not used because it has not been proven to be a reliable joining methodology [1, 2]. There have been instances where adhesive bonding was used reliably for several years, but then for unknown reasons began to produce low strength joints. The traditional method of dealing with a lack of reliability in metal structures is to use a nondestructive inspection (NDI) technique to detect the underlying cause of substandard performance and to alter the manufacturing or maintenance procedures to eliminate it. While NDI has proven to be a valuable asset in guaranteeing reliability in mechanical fastened structures, there has been no similar inspection capability that could detect low strength adhesive bonds. Without this fundamental capability composite materials could not be effectively utilized in high performance structures. In addition, without adhesive bonding as a joining option the composite structure can be more expensive than one fabricated from aluminum [1].

A brief history of bonded joint inspection

In the late 1990s the US Air Force began the Composite Affordability Initiative (CAI) to explore a number of approaches to reduce the cost and increase the reliability of aircraft components fabricated from carbon fiber reinforced polymers (CRFP). Several new technological approaches to achieving these goals were demonstrated during this program. One goal of the program was to make composite structural components economically competitive with mechanically fastened aluminum components. However, this can only be achieved if adhesive bonding can be used

R. L. Crane (✉)
200 Lewiston Rd., Kettering, OH 45429-2644, USA
e-mail: RCrane@woh.rr.com

G. Dillingham
Brighton Technologies Group, Inc., 1006 Kielely Place,
St. Bernard, OH 45217-1118, USA
e-mail: gdillingham@btgnow.com

as a reliable joining method. The principle conclusions at the end of the CAI effort as stated by the government engineer responsible for its conduct are—(1) “the key to affordability ... is the integration of parts and bonding parts” and (2) “The inability to discriminate between a good bond and a “kissing”¹ bond has been the key roadblock to further use of bonded structures” [1, 2]. Thus, adhesive bonding was identified as an enabling technology to the widespread use of composites in aircraft structures and the lack of a NDI capability to guarantee a minimum joint strength is fundamental to achieving both economical and reliable composite structures. The NDI community has long recognized the need for this inspection capability, and there have been a great many research programs over the years attempting to discover a method of “nondestructively measuring the strength of an adhesive bond.” A brief examination of those research efforts and the reason for their lack of success follows.

Nondestructive inspection has provided data about flaws and other strength limiting conditions of metal structures for well over 70 years using an array of instruments and techniques [3–12]. This information is conveyed to the engineering community and used in fracture mechanic analysis of structural performance and reliability. These flaw data and fracture mechanics analysis may provide the basis for recommended repair procedures. The combination of the analytical methods of fracture mechanics with reliable inspection data permits the engineering community to use the damage tolerance philosophy for both the design and maintenance of flight critical structures [13, 14]. At its core the damage tolerance philosophy assumes that all structures contain flaws at the time of fabrication whose sizes can be estimated from a quantification of the inspection capability of the manufacturer. Furthermore, these initial flaws will grow as a result of the service environment in a defined way so that service intervals for the structure may be determined in a quantifiable manner to guarantee safety of flight. Since the implementation of this philosophy, aircraft structures have been designed so that the initial flaws do not grow to critical size² during a specified service interval, if proper maintenance and inspection procedures are followed. The same formalism is applied to any service induced damage. Since its adoption by the US Air Force, the damage tolerance design philosophy has been eminently successful in guaranteeing the safe operation of large fleets of aircraft. Within the damage tolerance paradigm inspectors are charged with detecting and quantifying strength limiting flaws or material conditions, while the fracture mechanics community uses

these data to predict structural performance. Unfortunately, this paradigm was not applied to the inspection of bonded components where there has been an attempt to directly predict joint strength without the steps of detecting and quantifying strength limiting flaws [15–23]. In this case, the philosophy was to measure a physical parameter which was then correlated with bond strength. This process of NDI measurement and prediction evolved separately from that used in the damage tolerance philosophy for metal structures and we will examine why this occurred next.

NDI of bond strength

As early as the 1950s there was a great deal of interest in using adhesive bonding as a joining technique for aircraft structures. As the inevitable failures occurred with this new technology, there was increased pressure on the inspection community to develop a method to detect inadequate/under-strength bonds during the manufacturing process. In response to this need Fokker Aircraft in the Netherlands developed an instrument (the Fokker Bondtester) which seemed to be the universal answer to detecting substandard bonds during manufacturing [24–28]. This instrument was based upon two characteristics of the adhesive used by Fokker at that time. Firstly, the Redux adhesives [29] used by Fokker are forgiving of many deviations in surface treatments used to anodize aluminum components. Secondly, the principal defect of the Redux adhesive is excessive porosity. Fokker recognized that this condition could be detected with a low frequency acoustic instrument [25, 30–34]. The Fokker Bondtester measures the bandwidth or Q and resonant frequency of a small vibrating mass that is acoustically coupled to the structure. Since this coupling is via a viscous gel the instrument was not scanned but instead was used in selected locations with a suspect bond or one that sustains high stresses. Many later NDI research papers [25–27, 30–35] and the user’s manual for this instrument show graphs relating “bond quality units,” a meter reading on the instrument, with the strength of a lap shear joint. An example of such an image is shown in Fig. 1 for a lap shear joint.

Because the Fokker Bondtester provided strength estimates for adhesively bonded joints, it seemed to be the ideal solution to inspection bonds. The instrument was used from the 1960s through the 1990s to inspect many epoxy bonded structures, but the predictions of joint strength proved to be unreliable. The problem was principally due to a failure to recognize that the Redux adhesives and epoxies fail via different mechanisms. A Redux adhesive bond usually fails due to a lack of material or excess porosity. Epoxy bonds are sensitive to both the adherend surface condition and to small “crack like” flaws and fail

¹ A kissing bond is a one in which there is an intimate contact between adhesive and adherend but with little adhesion between them.

² A critical flaw is one that would initial brittle fracture.

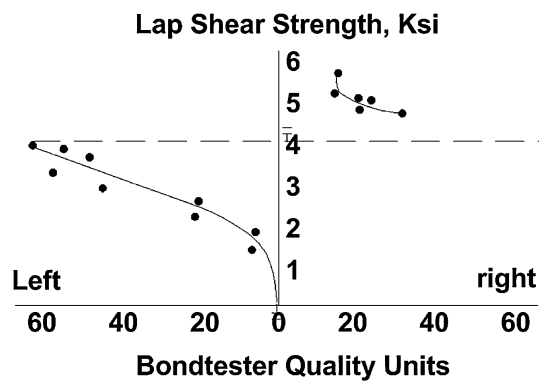


Fig. 1 Strength prediction using Fokker Bondtester for a lap shear joint with a Redux adhesive

via brittle fracture. Neither of these conditions is easily detectable using the Fokker Bondtester. Furthermore, the presence of cracks or “crack like” defects are not significant unless they are close to the edge of a joint where the stresses are highest [26–28, 36, 37]. Unfortunately, this is the region of the joint that is the least inspectable because the edge diffracts the relatively long wavelength acoustic waves and results in inconsistent signals. There have been several structural failures³ that were traced to bonded joints that had passed inspection with the Bondtester (R.N. Hadcock, 1997, Personal Communication). Nonetheless, a number of researchers have claimed that their data show that it is possible to measure the strength of adhesive bonds with the Bondtester. Others researchers have expanded their prediction capability to include a range of acoustic and ultrasonic methods. The most popular ultrasonic method uses through transmission ultrasound [15–17, 20–22, 38–77]. While the specifics of each of the ultrasonic techniques differ slightly, the basic configuration is similar to the through transmission configuration shown in Fig. 2. In this figure, two ultrasonic transducers are shown in contact with the specimen. The transducers are often separated from the specimen in a water bath that serves as an acoustic couplant. In this configuration, the specimen may be scanned in a raster pattern to provide the inspector with a planform image of internal voids and delaminations. Since the acoustic waves interact with the specimen at a normal incidence, longitudinal acoustic waves are used for this inspection configuration [6, 78].

As shown in Fig. 2 through transmission ultrasound is used to interrogate the joint in the middle, away from its edges. Near an edge diffraction of the sound waves can obscure sound reflected from small defects making their detection quite difficult. The important stress carrying regions at the edge of the joint therefore do not provide

³ Unfortunately references to such failures are rarely cited in the engineering and scientific literature.

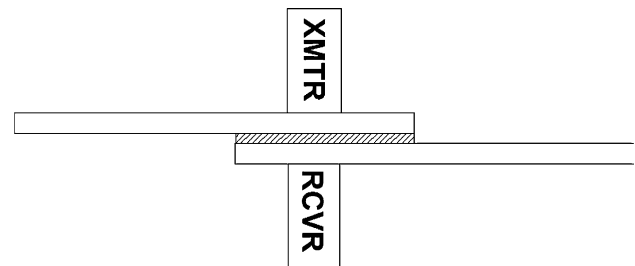


Fig. 2 A typical experimental setup for ultrasonic examination of a bonded lap-shear joint. XMTR is the transmitting transducer and RCVR is the receiving transducer for this through transmission configuration

much data to the inspector. This is unfortunate as it well known that for lap joint configurations, the edge of the adhesive joint carries nearly the entire load and therefore is the most sensitive region to defects. It is even possible to eliminate the central region of this joint without affecting the structural performance of the joint [37]. While this non-uniform stress distribution is well known in the mechanics community [79–83], its significance was not recognized by the NDI research community. Because of this omission the engineering design community cannot use NDI strength predicting correlations. The influence of the Fokker Bondtester based literature prejudiced many researchers to continue to pursue correlations using ultrasonic data for many years. Recently several NDI research groups have switched from predicting strength properties to predicting “bond quality” using the same ultrasonic data. Unfortunately, “quality” is not defined and progress was not forthcoming. Other types of ultrasonic inspection using different acoustic waves have been tried, but these too failed to produce a robust correlation between ultrasonic data and strength [84–98].

Proof testing

The other approach to estimating the strength of bonded joints is proof testing, wherein a “proof” load is applied to the structure that is either close to or even above the maximum load expected in service. If the joint fails, then under-strength joints are eliminated from service. Many methods of applying the proof load have been tried, including high power ultrasound, electron beam heating, plate impact, and electromagnetic pulses [69, 99]. Unfortunately, these methods suffered from two deficiencies. Firstly, the proof load is usually applied to a relatively large area and therefore has the potential of overloading areas not designed for such large loads. This is a problem associated with many proof load schemes since it is difficult to apply the load in a manner similar that is experienced in service. For example, the proof loads on an

aircraft wing are applied with pads and therefore not uniform in a manner similar to aerodynamic forces. This means that there will be high shear loads applied at the pads which are not present from aerodynamic loading. Secondly, the loads are applied at a slow rate so that the entire thickness of the specimen is stressed simultaneously and again a portion of the structure may be over stressed. A further difficulty of some proof loading schemes is the requirement for specialized facilities, e.g., a vacuum chamber in the case of electron beam heating. Plate impact loading requires precise alignment between plate and structure since a slight misalignment will mean that a very large overload will be applied along one edge at the plate-structure interface during the impact.

This was the state-of-the-art of adhesive bond inspection when a fortunate accident occurred to one of the authors in May 1996. During examination of several laser shock peened (LSP), high cycle fatigue test specimens with an ultrasonic microscope the author noticed that the LSP process had produced many very small delaminations in the center of the specimens. Images from one microscope scan are shown in Fig. 3 [100, 101]. This was a surprising result since no one had expected that the laser shock peening could fracture a specimen made from a high fracture toughness alloy, such as Ti-6Al-4V.⁴ Because the laser pulse can be as short as a few hundred nano seconds, the induced compressive and tensile pulses are on the order of several times the thickness of an adhesive bond. Furthermore, since the fluence of a high power laser can be accurately controlled the LSP process can be used to proof load a bond so that cohesive and adhesive strengths might be probed nearly independently.

The reason for the fractures or induced delaminations of the specimen shown in Fig. 3 may be explained as follows. During the LSP process a high power laser pulse is incident on specimen's surface and produce high amplitude compressional waves within the specimen. These compression waves reflect off the opposite free surfaces as tensile waves and overlap in its center to produce very large tensile loads that may fracture the specimen or bond—see Fig. 4 [101]. The resulting tensile stress may be nearly as large as twice the magnitude of each original compressive stress.

Proof loading of a joint in a small internal area therefore could then be used to fracture and thus detect low strength bonds. Substandard bonds will break and can be detected with standard ultrasonic scanning methods or by noting the deflection of the surface produced by the traversing stress pulses [102, 103]. If the area of the proof loading is small, then even if the bond is fractured, the structure may still meet acceptance standards. Furthermore, this interrogation method can be conducted in areas that carried little or no

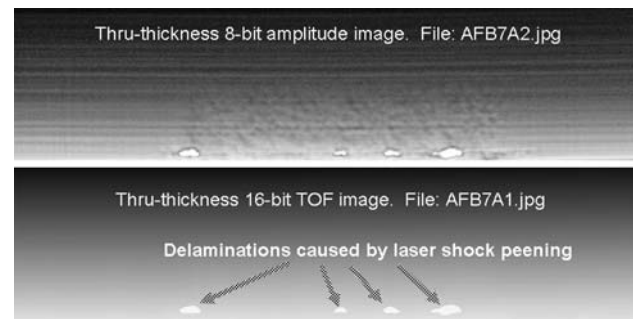


Fig. 3 Ultrasonic microscope images of a thin Ti-6Al-4 V specimen which had been laser shock peened to prevent high-cycle-fatigue crack growth

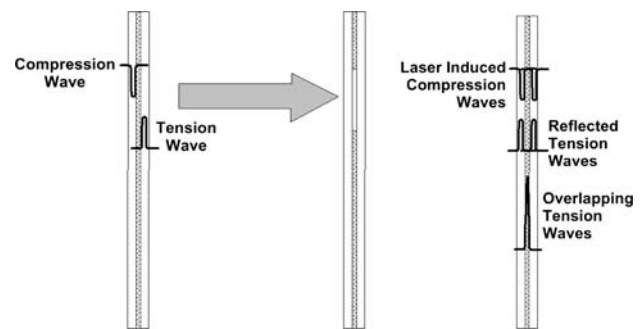


Fig. 4 A schematic explanation of why laser shock peening produces a large tensile stress at the center of a bonded composite specimen [101]

load, e.g., far from the joint edge, and thus would not be detrimental to joint integrity or durability. One aircraft structural designer has suggested that these small delaminations are the equivalent of an insignificant increase in the amount of porosity that is assumed to be present in all adhesive bonds (M. Pourmand, 2001, Personal Communication Northrop-Grumman Corp.).

Current certification requirements for primary bonded structures, as mandated by the US Federal Aviation Administration and the US Department of Defense, require proof testing to ensure adhesive joints meet minimum strength levels. Unfortunately, conventional proof testing is often too costly to be used on a routine basis. However, using LSP to proof load a small area avoids these difficulties since only a small fraction of the structure is loaded and even if a fracture occurs, it is unlikely to be significant from a structural standpoint. This latter point has not been proven with long-term structural testing and is only the opinion of one structural engineer (M. Pourmand, 2001, Personal Communication Northrop-Grumman Corp.). Based upon these findings, work on laser shock loading of adhesive joints in composite specimens was continued and expanded under the CAI program, and is reviewed next [99, 102, 103].

⁴ A titanium alloy with 6% aluminum and 4% vanadium.

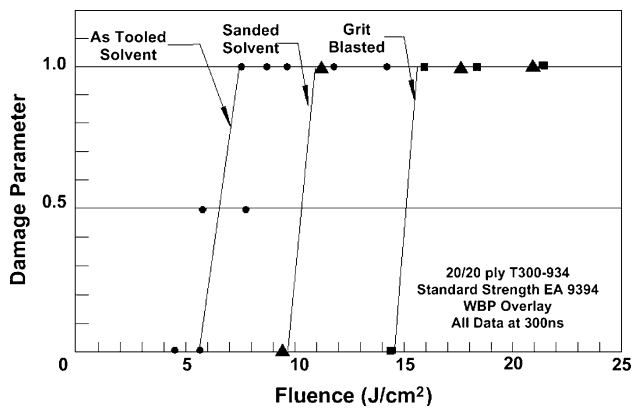


Fig. 5 Effect of surface preparation on the adhesive strength of bonded composite specimens as detected with laser shock peen proof loading. The circles represent strength data for specimens without any surface treatment before bonding, while the triangles represent strength data for specimens which had been sanded and wiped with a solvent. The small squares represent strength data from specimens which had received grit blasting before bonding. Used with permission [103] “Reprinted by permission from the Society for the Advancement of Material and Process Engineering (SAMPE)”

Specimens were fabricated with Cytec Fiberite 3 K-70-PW T300 934 graphite/epoxy composite material and Loctite Hysol EA 9394 adhesive bonds—for further details of the specimen preparation see [103]. The surfaces of several specimens were prepared using three different techniques to determine if these changes could be detected with the LSP proof loading. The methods of treating the adherent surface were as follows: (1) “as-tooled” or untreated after consolidation; (2) sanded and wiped with a solvent; and (3) grit blasting. These samples were LSP proof tested and the results showed that these conditions could be distinguished by their different adhesive strengths with the untreated, sanded and solvent wiped, and grit blasted specimens having progressively higher adhesive strength levels—see Fig. 5. The damage parameter shown on the ordinate was assigned to the tested specimen in the following manner. Specimens without detectable delaminations, determined with ultrasonic C-scanning [78], were classified as having no damage. Those with barely discernable delaminations at the LSP impact site were classified as having a damage parameter of 0.5, while those with clear delaminations were classified as having damage levels of 1.0.

To test the ability of the proof loading to distinguish between adhesives of differing cohesive strength levels, the EA 9394 paste epoxy was mixed with various ratios of resin and hardener. Three differing levels of strength were achieved with static cohesive strength levels of 50%, 70%, and 100%. Again these were easily detected with the LSP proof testing—see the results in Fig. 6.

Lastly, there was an attempt to determine if contamination could be detected with the LSP proof testing.

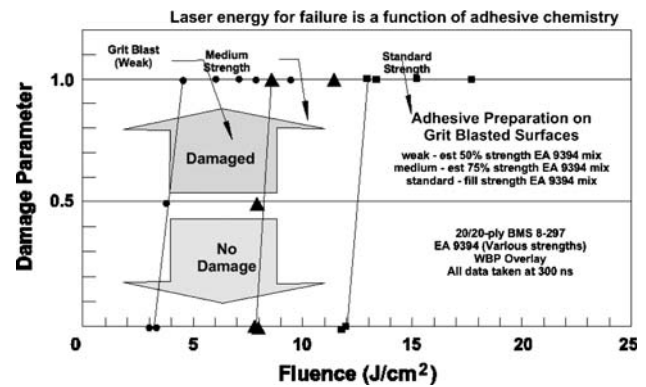


Fig. 6 Effect of the adhesive resin-hardener ratio on the cohesive strength of bonded composite specimens as detected with laser shock peen proof loading. The circles represent strength data for specimens which had been bonded with an adhesive (EA 9394) with insufficient hardener so as to yield 50% strength joints. The triangles represent strength data for specimens with a 75% strength adhesive and the squares represent strength data from specimens prepared with full strength adhesive. Used with permission [103] “Reprinted by permission from the Society for the Advancement of Material and Process Engineering (SAMPE)”

Composite adherents were prepared with the standard processing and the surfaces were then grit blasted. The bondline surfaces were then intentionally contaminated with two levels of Frekote 1711. One set of specimens was left uncontaminated as a control group. As expected, contamination degraded the adhesive strength, and this is apparent from the LSP proof loading as shown in Fig. 7.

The data shown in Figs. 5–7 indicate that LSP proof loading can be used to detect differences in the adhesive and cohesive strength of bonded composite specimens.

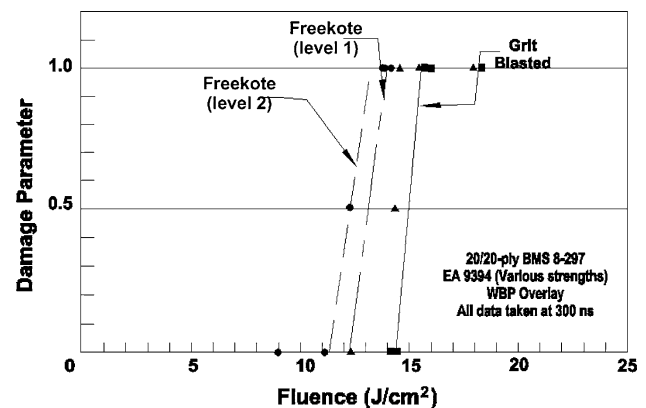


Fig. 7 Effect of contamination by Frekote 1711 on the adhesive strength of bonded composite specimens as detected with laser shock peen proof loading. The circles represent strength data for specimens with the greatest surface contamination with Frekote 1711, while the triangles represent strength data for specimens with a lesser amount of contamination. The squares represent strength data from specimens which had received only grit blasting. Used with permission [103] “Reprinted by permission from the Society for the Advancement of Material and Process Engineering (SAMPE)”

This method is significant because it detects a parameter that is directly related to the strength of the bond joint. It should be noted that the ultimate load bearing capability of the complete structure is not probed with this technique because the defect distribution at the edges of the joint is not probed. However, the method does detect the existence of under-strength bonds and permits the inspector to cull those with substandard adhesive or cohesive strengths.

Proof loading conclusions

At this point one may draw several conclusions. Firstly, a method has been found to test the fracture/strength properties of an adhesive bond in situ. This capability is a necessary component of the inspection process in order for aircraft designers to have confidence that adhesive bonding can be used reliably as a joining method for composite structures (W.G. Baron, 2001, Personal Communication Air Force Research Laboratory, Air Vehicles Directorate, Wright Patterson AFB, OH 45433). Secondly, while this is a destructive test procedure, which the NDI community may choose to exclude from their repertoire of tools. However, it is similar to acoustic emission in that minor physical damage is done to the structure during the testing procedure.⁵ This does not seem to be a major concern for aircraft designers who consider any small delaminations induced by LSP proof loading to be equivalent to a slight increase in the porosity that is assumed to exist in all adhesive bonds. Furthermore, these delaminations may be created in the area of the joint that effectively carries little or no load, so their presence may be of little or no consequence to the strength and durability of the joint. Thirdly, this technique will probably never be used over large areas of a bond due to cost and time involved in its application. Therefore, traditional inspection techniques must be utilized to detect and quantify physical flaws, such as delaminations, excess porosity, inclusions, missing adhesive, etc. These flaw types must be detected in high stress areas of the structure where their presence is significant to the reliability of a bond. Finally, this technique is expensive and is applied late in the manufacturing cycle, i.e., after the part has been assembled and the adhesive cured. Since a common cause of low adhesive strength is contamination or improper surface preparation of the adherend surface before the adhesive is applied, if a method of detecting these conditions could be found, then these parts could be reworked and the components salvaged. If contamination can be detected before adhesive application,

then the source of contamination might be discovered and eliminated.

NDI for contamination detection

In the 1970s the US Air Force conducted a program called “Primary Adhesively Bonded Structural Test” (PABST) to determine if adhesive bonding could be used reliably as a joining method for the primary components in aluminum airframes⁶ [104–107]. During this program a great deal of attention was given to all aspects of the manufacturing process that could affect the long-term durability of an adhesively bonded joint. A review of previous failures and those that occurred during the PABST program indicated that most were traceable to inadequate surface preparation of the anodized aluminum prior to priming and adhesive application. There were a few failures traced to physical flaws, such as delaminations but most were associated with contamination or damage to the adherent surface.⁷ As a result, particular attention was paid to prevention of contamination of the anodized aluminum surface with rigid process controls. In addition, several research efforts were initiated to discover and develop a method and/or device that could detect the presence of contamination on anodized aluminum [108–116]. The conclusions reached at the end of these efforts may be summarized as follows. Firstly, all surfaces are contaminated with a non-native material. Extraneous substances are present in the environment and many condense on the surface of the anodized components before it is primed. Secondly, almost all of these contaminants are benign since most are soluble in the adhesive during curing. Only a few contaminants are pernicious, e.g., silicone greases used in the pumps that circulate the hot anodizing fluids. Thirdly, there are several physical measurements capable of detecting a foreign substance on the surface of the aluminum components [35, 108–115, 117–129]. While several instruments were quite effective at detecting contamination, none could easily or quickly distinguish between benign and pernicious contaminants. Therefore, instead of using an instrument to detect contamination, rigid process controls were instituted in an attempt to eliminate the damaging contamination. While the importance of surface condition is recognized as the key to adhesive bonding [1, 2, 116, 127, 128, 130–133], no technique has yet emerged that can detect the presence and chemical character of surface contamination.

⁵ The data recorded during acoustic emission testing is generated by many sources including the extension of previously existing cracks and/or the generation of new flaws.

⁶ The test article chosen for this program was the C-17 fuselage.

⁷ It is possible to physically damage the oxide on the anodized surface and significantly degrade the adhesive bond strength, but this seemed to be a rare condition.

Surface energy and adhesion

One area of technology that is particularly well equipped to both detect and characterize contamination is the science of surface chemistry. Previous work in this field has demonstrated that surface energy measurements are an excellent predictor of adhesive bond performance [118, 134–136]. However, the measurement of solid surface energies using contact angle techniques is time consuming and tedious, particularly for non-ideal surfaces, such as those that are curved and in a non-horizontal position. However, the adhesion of pressure sensitive adhesive (PSA) tapes to a surface is a function of surface energy, and peel strength measurement could be used as a predictor of adhesive bond performance, even on highly roughened surfaces. Therefore, a research effort was initiated to investigate the relationship between surface energy, the work of adhesion, and peel strength of pressure sensitive tapes on epoxy/carbon fiber composite laminates as a function of a limited range of surface conditions.

Adhesive tapes are based on PSAs and fall into two main classes: (1) natural rubber (cis-polyisoprene) and (2) acrylic copolymers, commonly either butyl, or 2-ethylhexyl acrylate and acrylic acid. Masking tapes tend to use natural rubber-based compounds, while the familiar plastic-backed Scotch-type tapes frequently use acrylic formulations. This study utilized two PSA tapes—one based upon an acrylic adhesive (Loparex 974660) and one based upon a natural rubber adhesive (3M #200).

Adhesion of a PSA tape to a surface may be predicted using a rheological model [136–138]:

$$G = W_a \Phi(v, T) \quad (1)$$

where G is the peel adhesion strength, W_a is the thermodynamic work of adhesion, Φ is the rheological loss in the adhesive during peel, v is the peeling velocity, and T is the temperature. Because of the viscoelastic nature of PSAs, Φ can be larger than W_a . However, at low peel rates and/or low temperatures, $\Phi \rightarrow 1$ and $G \rightarrow W_a$. Therefore, the work of adhesion may be related to the surface energy between the adhesive and the adherend or substrate.

The relationship between the surface energy of the substrate, γ_{sv} , the surface energy of a liquid in contact with its vapor, γ_{lv} , and the energy of the liquid/substrate boundary, γ_{sl} , is shown schematically in Fig. 8.

Accounting for all the surface energy terms, the Young Eq. (2) may be easily derived.

$$\gamma_{sv} = \gamma_s - \pi_s = \gamma_{lv} \cos \theta + \gamma_{sl} \quad (2)$$

where γ_s is the true surface energy of the substrate, π_s is the spreading pressure of the liquid, and θ is the contact angle between the liquid and the substrate. Usually π_s is set to 0 for solids, and with γ_{sv} being equal to γ_s , a simpler

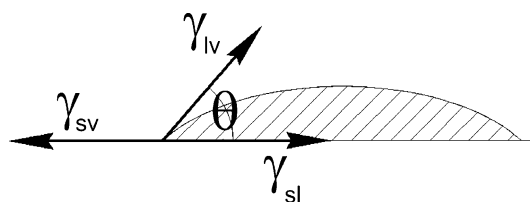


Fig. 8 A schematic representation of the Young diagram and the surface energy relationships for a liquid drop on a solid substrate

relationship and more familiar Young equation is obtained. γ_{lv} is usually known because a standard liquid is used for the drop and θ is measured experimentally [139]. In order to determine γ_s , the energy of the solid/liquid interface, γ_{sl} must also be known. For this purpose the linearized Kaelble equation for γ_{sl} is applied [140].

$$\gamma_{sl} = \gamma_s + \gamma_{lv} - 2(\gamma_s^d \gamma_{lv}^d)^{1/2} - 2(\gamma_s^p \gamma_{lv}^p)^{1/2} \quad (3)$$

where γ_{lv}^d is the dispersive component of the liquid–vapor energy and likewise the term γ_{lv}^p is its polar component. Equation 3 assumes surface energies of both the liquid and solid have been separated into their constituent dispersion and polar forces. This separation is shown explicitly for the liquid–vapor surface energy by Eq. 4.

$$\gamma_{lv} = \gamma_{lv}^d + \gamma_{lv}^p \quad (4)$$

If Eq. 3 is substituted into Eq. 2, a relationship between the contact angle and the dispersive and polar components of the surface energies of the liquid and solid is obtained.

$$\cos \theta = -1 + \frac{[2(\gamma_s^d \gamma_{lv}^d)^{1/2} + 2(\gamma_s^p \gamma_{lv}^p)^{1/2}]}{\gamma_{lv}} \quad (5)$$

By measuring the contact angle of a liquid with a liquid of known surface energy $\gamma_{lv} = \gamma_{lv}^d + \gamma_{lv}^p$ and substituting this value into Eq. 5 a single equation is produced with two unknowns, γ_s^d and γ_s^p . To determine these two unknowns, it is necessary to measure the contact angle of a second liquid with well-characterized surface properties. These two equations may then be solved for the two unknowns γ_s^d and γ_s^p , yielding a more complete description of the surface energetics of the solid surface.

The relationship between work of adhesion of Eq. 1 and the surface energies of the adhesive, γ_a^d and γ_a^p , and substrate, γ_s^d and γ_s^p , is given by Eq. 6.

$$G \rightarrow W_a = 2(\gamma_a^d \cdot \gamma_s^d)^{1/2} + 2(\gamma_a^p \cdot \gamma_s^p)^{1/2} \quad (6)$$

Using Eq. 6 and noting that G is related to W_a , which is directly related to the surface energies of the substrate, the peel strength of an adhesive may be predicted if the surface energies of the adhesive and substrate are known. Conversely, the surface energy of the substrate may be determined from the peel strength of a standard PSA. In most inspection processes, it is only necessary to detect a

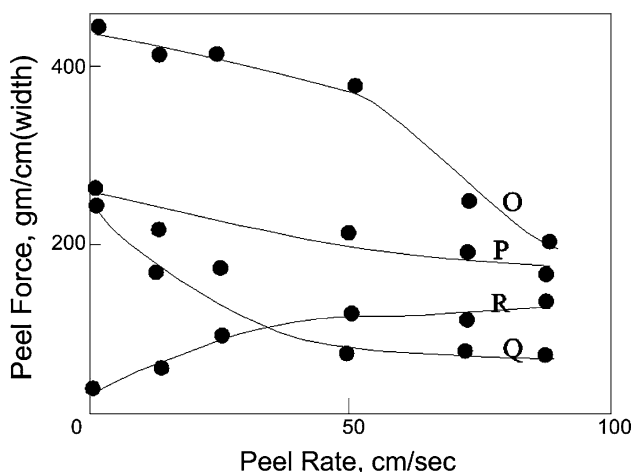


Fig. 9 Effect of release coatings on peel strength of a pressure sensitive adhesive for several peel rates. (O) Acrylic release coating; (P) Quilon C release; (Q) polyethylene release coating; (R) silicone release coating. From [142]

change in material properties from a standard state. Since a change in the surface energies of the substrate may be detected from the peel strength of a standard adhesive, a simple peel test should be a sensitive indicator of surface condition. Therefore this test should be capable of detecting surface conditions that are deleterious to adhesive bond strength, such as improper preparation and/or contamination with a substance incompatible with the adhesive.

While in practice the threshold values for G are 100–1,000 times larger than W_a , the correlation between G and W_a is well known. For example, acrylic PSAs are known to adhere more strongly to polar surfaces than rubber-based PSAs, but less strongly to non-polar surfaces, such as polyethylene [141]. For example, polar acrylics may exhibit 50% lower peel adhesion to polyethylene than to steel [142].

In addition to a correlation with surface energy of the substrate, peel strength of a PSA has been shown to correlate well to the presence of contaminants that affect bond strength [142]. Figure 9 shows the relationship between peel force and peel rate for surfaces coated with various release coatings. The reader will note that the effect of contamination on peel strength is much greater at low peeling rates. This validates Eq. 1, which indicates a much greater role of the thermodynamic work of adhesion at low rates where viscoelastic energy dissipation is at a minimum.

Experimental procedure

The PSA tape and an application roller, used for a paint adhesion test (ASTM D2510), were used to ensure reproducible application of the tape to the laminate surfaces. The peel testing apparatus shown in Fig. 10 consists of a motor-driven sample stage and a force gauge. The tape was peeled

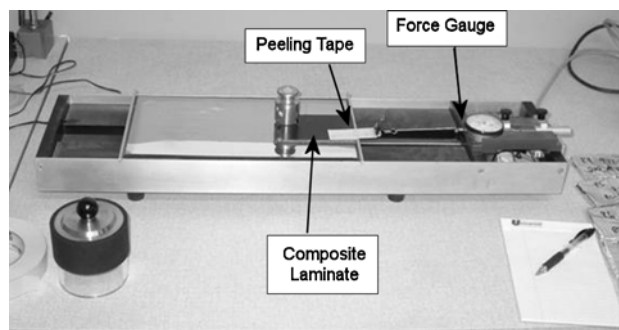


Fig. 10 Apparatus used for evaluating the 180° tape peel strength of pressure sensitive adhesive tapes on a composite surface

from the composite surface at a 180° angle and a rate of 2.54 mm/s. The 180° peel test is a much simpler configuration to instrument than a 90° peel test, which requires the force gauge to follow the advancing peel interface between the tape and substrate.

Table 1 shows the types of adhesive tapes acquired for this investigation. Infrared spectroscopy indicated all the tapes except the 3M #200 had very similar acrylic polymer PSA composition. The PSA on the 3M #200 was an aliphatic rubber. The surface energies of the Loparex 974660 and the 3M #200 were determined using the linearized Kaelble approach [140]. Surface energies cited in this study were determined with the proof liquids listed in Table 2. All surface energies are in mJ/m^2 .

Laminates were evaluated as-received, with no additional cleaning attempted. Tape was applied to one edge of the laminate and the rubber-coated roller, with a force of 20 Newtons. The roller was rolled four times back and forth (eight total passes) over the tape. The force in Newtons required to remove the tape was divided by the tape width to obtain the peel strength. In some cases, the tape peel tests were repeated several times by re-applying a fresh piece of tape to the area previously evaluated and the debris present on the peeled tape evaluated with a stereo microscope. Table 3 shows the panels evaluated for peel strength.

Figure 11 shows a series of grit blasted laminates that had PSA tape applied and removed either once, twice, thrice, or a maximum of four times. The reader will note that with each successive tape peel less grit blast debris was left on the surface of the specimen. When viewed under higher magnification the presence of debris was more dramatic.

The peel energy for the initial tests fluctuated widely as the test progressed, but subsequent peel tests showed much more stable peel energy data as the test progressed. However, the average peel energy remained consistent for multiple tests with remarkably little variation in the average strength from test to test. Grit blast debris seemed to have very little effect on the average peel strength even

Table 1 Adhesive tapes used as surface probes

| Tape | Type | Adhesive | Surface energy | | |
|----------------|----------------------|---------------------|----------------|------------|------------|
| | | | γ^d | γ^p | γ_s |
| 3M #600 | Packing | Acrylic | | | |
| 3M #2090 | Safe-release masking | Synthetic | | | |
| Loparex 974660 | High-tack masking | Acrylic | 29.9 | 2.4 | 32.3 |
| Loparex 591260 | Low-tack masking | Acrylic | | | |
| 3M #200 | X-hatch masking | Natural rubber base | 35.9 | 0.14 | 36.0 |

Table 2 Liquids used for determination of solid surface energies

| Proof liquid | Dispersive | Polar |
|--------------------------------|------------|-------|
| Glycerol | 34.0 | 30.0 |
| Water | 22.0 | 50.2 |
| Ethylene glycol | 29.3 | 19.0 |
| DMSO | 34.9 | 8.7 |
| CH ₂ I ₂ | 48.5 | 2.3 |
| Formamide | 32.3 | 26.0 |
| Tricresylphosphate | 36.2 | 4.5 |

Table 3 Panels used in tape peel tests

| Surface type | γ^d | γ^p | γ_s | Surface roughness (R_a) |
|--|------------|------------|------------|-----------------------------|
| S1 as-tooled | 35.5 | 4.6 | 40.1 | 20 |
| S2 as-tooled | 35.6 | 4.6 | 40.3 | 20 |
| S3 150 hand sanded | 40.1 | 9.6 | 49.6 | 50 |
| S4 220 garnet blast media | 39.4 | 11.3 | 50.7 | 148 |
| S5 220 blast media Al ₂ O ₃ | 39.6 | 11.6 | 51.1 | 40 |
| S6 as-tooled | 35.2 | 0.3 | 35.5 | 18 |
| S7 as-tooled | 32.6 | 1.0 | 33.6 | 18 |
| S8 150 hand sanded | 38.2 | 12.7 | 50.9 | 47 |
| S9 220 blast media garnet | 40.1 | 8.8 | 48.9 | 156 |
| S10 220 blast media Al ₂ O ₃ | 41.2 | 7.2 | 48.4 | |

with a relatively large amount of debris present on the laminate. If an adhesive has low fracture toughness, then the joint might be more sensitive to the blast debris that could serve as crack initiators. However, due to their viscoelastic nature PSAs have a higher toughness and therefore are relatively insensitive to debris, which had little effect on peel strength of the tape.

The force required to remove PSA tape from a surface is usually considered to increase with increased surface roughness, if for no other reason than higher roughness surfaces have greater surface area. To test the sensitivity of the tapes used in this study to surface roughness, the values of peel strengths are plotted as a function of surface roughness as shown in Fig. 12. There seems to be a very little correlation between roughness and peel strength for the tapes used in this study—an acrylic adhesive (Loparex

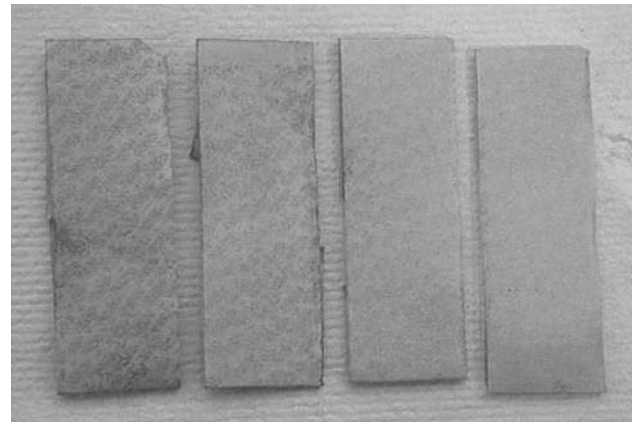


Fig. 11 Surfaces of composite specimens after removal of a pressure sensitive tape. The composite has been grit blasted with 80 grit garnet. Tape from first peel is on the left, with the second and third and fourth tape peels shown progressively to the right. Note that less debris remains on the composite surface after each application of the tape and its removal

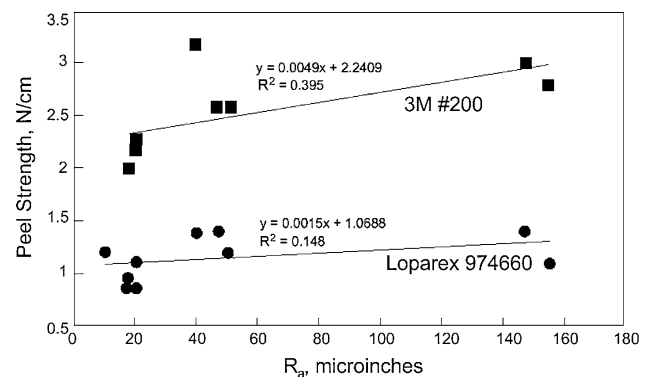


Fig. 12 Pressure sensitive adhesive tape peel strengths plotted as a function of surface roughness

974660) and one based on natural rubber adhesive (3M #200).

Figure 13 shows strong correlation between peel strength and total surface energy for composite specimens. This plot shows that a tape peel measurement has strong potential as a probe of surface energy. The governing equation for peel strength involves the work of adhesion, not the total surface energy. W_a (see Eq. 6) is only

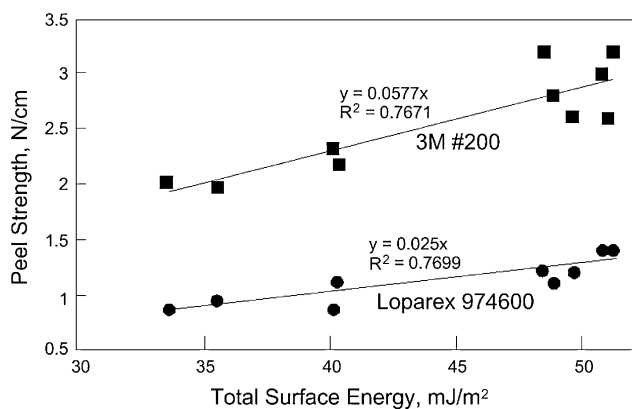


Fig. 13 Peel strength for pressure sensitive adhesive tape plotted as a function of total surface energy

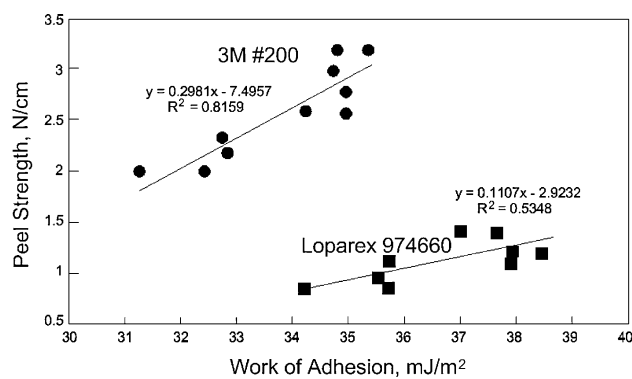


Fig. 14 Peel strength for pressure sensitive adhesive tape plotted as a function of the thermodynamic work of adhesion (W_a)

indirectly related to the total surface energy ($\gamma_s^d + \gamma_s^p$). But as seen in Fig. 14, correlation of the peel strength to the work of adhesion is no better and, in the case of the acrylic PSA, not as strongly correlated.

Tape peel tests were performed on as-grit blasted as well as contaminated composite surfaces to determine if peel strength is sufficiently sensitive to surface energy to be used as a contamination detection tool. Composite laminate samples were first grit blasted with 220 grit alumina using N_2 at a pressure of 2.4 bars. Care was taken to uniformly roughen the surface without removing the resin cap over the first ply fibers. A control sample was left in the as-grit blasted condition, while other samples were contaminated to different levels with solutions of Frekote 44, a cross-linkable mold release material. Contaminated samples were cured in a 125 °C oven for 15 min as per Frekote 44 instructions. Surface energy and DMSO⁸ drop diameter

⁸ DMSO is dimethyl sulfoxide (DMSO) a liquid commonly used as surface energy standard. See http://en.wikipedia.org/wiki/Dimethyl_sulfoxide or http://www.vp-scientific.com/hydrophobic_coating.htm for more information about this substance.

Table 4 Dispersive (γ_s^d), polar (γ_s^p), and total (γ_s^t) surface energy of contaminated composite laminate samples used for PSA tape peel adhesion test

| Time in spray (s) | γ_s^d (mJ/m ²) | γ_s^p (mJ/m ²) | γ_s^t (mJ/m ²) |
|-------------------|-----------------------------------|-----------------------------------|-----------------------------------|
| Saturated | 14.53 | 1.12 | 15.66 |
| 3.0 | 43.38 | 0.48 | 43.87 |
| 1.5 | 47.76 | 0.75 | 48.51 |
| 0 | 44.21 | 6.10 | 50.31 |

measurements⁹ were made on one end of samples, and PSA tape peel tests were performed on the other end.

3M 250 Flatback Masking tape (with a natural rubber PSA adhesive) was applied using 8 passes with a 2 kg roller to obtain a reproducible tape application to the laminate surface. 180° peel tests were performed using a motor-driven device at a rate of 2.54 mm/s. Surface energy measurements and drop diameters of a standard liquid, DMSO were obtained. A calibrated pipette was used to place 3 μ L drops of DMSO on the surface of the composite and the diameters of each drop measured after it had spread to its maximum extent. Table 4 lists the contaminated composite surface energies as determined by a linearized Kaelble analysis [140].

Results from tape peel tests of these surfaces are shown in Fig. 15.

These data show a strong dependence of tape peel strength on surface energy for grit blasted epoxy laminates. The correlation seems to be stronger for surface energies below about 40 mJ/m². The amount of contamination present on these higher energy surfaces may not have been sufficient to affect peel strength.

DMSO drop diameter was similarly a good predictor of peel strength, as shown in Fig. 16.

For drop diameters up to approximately 4.5 mm, the correlation with peel strength is particularly strong. For larger DMSO drop diameters (corresponding to surface energies > 43 mJ/m²), peel strength reached a maximum of approximately 4.4 N/cm. The relationship between PSA adhesion and surface energy suggests that this technique could form the basis of a tool for measuring surface energy and thus to gauge readiness of a grit blasted composite surface for adhesive bonding.

As these results suggest, either the DMSO drop or the tape peel test could be utilized to detect the presence of at least one type of common contaminant on composite surfaces before bonding. It must be noted that only a limited range of contamination levels was investigated during this study. Furthermore, while a mold release compound, such as Frekote 44 is a likely contaminate in a composite

⁹ The diameter of a drop with a specified volume is directly related to the contact angle between the drop and the substrate.

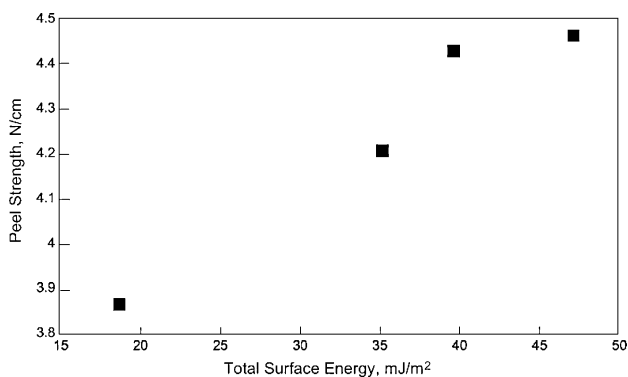


Fig. 15 A comparison of peel strength as measured for pressure sensitive adhesive tape peel test vs. the surface energy as determined by multiple liquid contact angle method

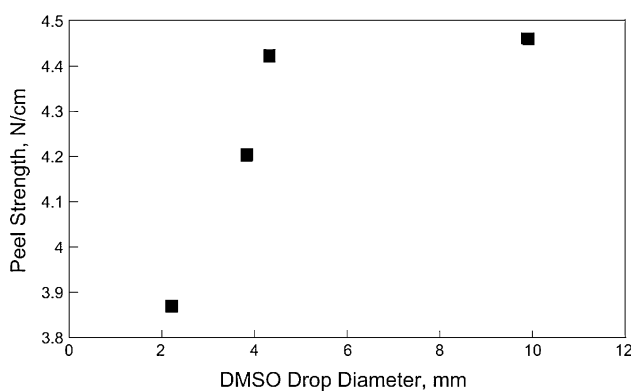


Fig. 16 A comparison of peel strength as measured for pressure sensitive adhesive tape peel test vs. the drop diameter of 3 μ L DMSO drops

fabrication facility, it is not the only one. With many possible contaminants available in any modern manufacturing facility, further testing and evaluation needs to be conducted before the likelihood of detecting pernicious contaminants is proven. Furthermore, since only one type of pernicious contaminant was included in the test matrix, additional testing will be necessary to demonstrate that this method can distinguish between the many types of contaminants that could affect bond strength and durability.

While the drop test appears to be more sensitive to changes in peel strength, particularly at low surface energies, this could prove to be a difficult procedure to implement in a production environment. One can easily conceive of many inexpensive, simple mechanical implementations of a tape peel test that would be fast and easy to apply in a fast paced environment of the production floor.

Conclusions

The general conclusion from the work discussed in this paper is that the Holy Grail of adhesive bond NDI has been

found [143]. It is now possible, albeit expensive (CT Walters, 2007, Personal Communication 6145 Scherers Pl, Ste F, Dublin, OH 43016-1284), to provide the structural engineer with a direct measurement of a strength property of an adhesive joint. This is crucial information for structural designers as it enables them to perform hitherto unfeasible deterministic design for bonded composite structures. In addition, this design approach allows the designer to significantly reduce the weight of composite aircraft structures. However, LSP proof testing has several limitations, including the need for access to two surfaces and the high expense of the instrumentation. However, given the importance of weight savings in transport structures and the need to assure structural reliability of bonded composite joints, this approach to determining joint properties in situ seems justifiable for weight critical applications.

During the fabrication steps before the final assembly of a composite structure, a major concern for the NDI engineer is the detection of pernicious contamination. The tape peel test offers an approach that is potentially inexpensive and could be implemented in a fast paced production environment. Unfortunately, there is insufficient data at this time on a wide range of possible contaminants and the possible levels of concentration for this approach to be rapidly applied. However, it does offer an approach to providing the NDI engineer an important tool to access the adhesion potential of a composite surface before the consolidation of a component.

References

- Russell JD (2007) SAMPE J 43:26
- Russell JD (2007) AMMATIC 1:1
- Stanley RK (1995) Special nondestructive testing methods, 2nd edn. Am. Soc. Nondestruct. Test., Columbus
- Schmidt JT, Skeie K (1989) Magnetic particle testing, 2nd edn. Am. Soc. Nondestruct. Test., Columbus
- Allgaier MW, Ness S (1993) Visual and optical testing, 2nd edn. Am. Soc. Nondestruct. Test., Columbus
- Birks AS, Green JRE (1991) Ultrasonic testing, 2nd edn. Am. Soc. Nondestruct. Test., Columbus Ohio
- Bryant LE (1985) Radiography and radiation testing, 2nd edn. Am. Soc. Nondestruct. Test., Columbus
- Jackson CN, Sherlock CN (1998) Leak testing, 3rd edn. Am. Soc. Nondestruct. Test., Columbus
- McMaster RC (1982) Liquid penetrant testing, 2nd edn. Am. Soc. Nondestruct. Test., Columbus
- Mester ML (1986) Electromagnetic testing, 2nd edn. Am. Soc. Nondestruct. Test., Columbus
- Miller RK (1987) Acoustic emission. Am. Soc. Nondestruct. Test., Columbus
- McMaster RC (1959) The nondestructive testing handbook. Ronald Press, New York
- Hertzberg RW (1995) Deformation and fracture mechanics of engineering materials. Wiley, New York
- Grandt AF Jr (2003) Fundamentals of structural integrity: damage tolerant design and nondestructive evaluation. Wiley-Interscience, New York

15. Alers GA (1977) AFML-TR-77-44 Air Force Materials Laboratory
16. Alers GA et al (1978) Proceedings of the ARPA/AFML Review of progress in quantitative NDE 191 Air Force Materials Laboratory, Wright Patterson Air Force Base OH
17. Mal AK, Bar-Cohen Y (1989) International conference on fatigue-7: advances in fracture research, vol 5. Pergamon Press, New York, p 3197
18. Rose JL (1976) Durability of adhesive bonded structures. Wiley, New York, p 561
19. Rose JL, Thomas GH (1980) ASNT National Spring Conference, Society for Nondestructive Testing, Columbus, p 184
20. Saffari N (1990) Rev Prog Quant Nondestruct Eval, vol 10B. Plenum, p 1335
21. Singher L (1997) NDTnet 2
22. Singher L (1997) Ultrason 35:305. doi:[10.1016/S0041-624X\(96\)00109-6](https://doi.org/10.1016/S0041-624X(96)00109-6)
23. Wegman F, Mitchell JR (1989) Advanced materials: the Big Payoff 196 SAMPE, Covina
24. Evans GB (1965) Sheet Met Ind 42:751
25. Schliekelmann RJ (1965) Metlaen 20:330
26. Smith DF, Cagle CV (1966) Mater Eval 24:362
27. Botsco R, Roopenian R (1968) Mater Eval 26:90
28. Gorbunov A (1968) Sov J Nondestruct Test 2:42
29. Redux (adhesive) (2007) [http://en.wikipedia.org/wiki/Redux_\(adhesive\)](http://en.wikipedia.org/wiki/Redux_(adhesive)). Accessed 11 Nov 2007
30. Schliekelmann RJ (1972) Nondestruct Test 5:144. doi:[10.1016/0029-1021\(72\)90032-1](https://doi.org/10.1016/0029-1021(72)90032-1)
31. Schliekelmann RJ (1972) Nondestruct Test 5:79. doi:[10.1016/0029-1021\(72\)90099-0](https://doi.org/10.1016/0029-1021(72)90099-0)
32. Schliekelmann RJ (1975) Recent Dev Test Sys Nondestruct Test 8(2):100
33. Schliekelmann RJ (1975) Nondestruct Test 8:100. doi:[10.1016/0029-1021\(75\)90161-9](https://doi.org/10.1016/0029-1021(75)90161-9)
34. Schliekelmann RJ (1979) AGARD Lecture series, bonded joints and preparation for bonding, vol LS-102. p 37
35. Brockmann W (1970) Aerospace Adhesives and Elastomers 477 SAMPE, Covina, CA
36. Schonhorn H et al (1971) J Appl Appl Polym Sci 15:1069. doi:[10.1002/app.1971.070150503](https://doi.org/10.1002/app.1971.070150503)
37. Wang TT et al (1972) J Appl Appl Polym Sci 16:1901. doi:[10.1002/app.1972.070160804](https://doi.org/10.1002/app.1972.070160804)
38. Thompson DO et al (1974) Mater Eval 32:81
39. Alers GA et al (1977) Mater Eval 35:77
40. Alers GA, Elsley RD (1977) Ultrasonics symposium proceedings 35 institute of electrical and electronic engineers (IEEE), Piscataway
41. Buckley MJ, Raney JM (1977) AFRL-TR-77-55 Air Force Materials Laboratory
42. Flynn PL (1977) AFML-TR-77-44 Air Force Materials Laboratory
43. Meyer PA, Rose JL (1977) J Appl Phys 48:3705. doi:[10.1063/1.324285](https://doi.org/10.1063/1.324285)
44. Alers GA et al (1978) Rev Prog Quant Nondestruct Eval. Plenum Publishing, New York, p 266
45. Alers GA, Elsley RK (1979) Structural adhesives and bonding technology conferences association, El Segundo, CA, USA, p 119
46. Mazurek J et al (1979) Ninth World Conference on Non-Destructive Testing 8 Australian Institute of Metals, Melbourne
47. Rose JL, Thomas GH (1979) Br J Nondestruct Test 3:135
48. Pilarski A, Pawlowski Z (1979) Ninth world conference on non-destructive testing. Australian Institute of Metals, Melbourne, p 8
49. Kapoor A, Prakash R (1984) Advances in fracture research (fracture 84), vol 4. Pergamon Press Ltd., New Delhi, p 2649
50. Hagemaiier D (1985) In: Thrall EW, Shannon RW (ed) Adhesive bonding of aluminum alloys. Marcel Dekker Inc., New York, p 337
51. Reis HLMD et al (1986) Br J Nondestruct Test 28:357
52. Reis HLMD, Krautz HE (1986) J Acoust Emission 5:144
53. Pilarski A et al (1987) Acousto-ultrasonics: theory and application. Plenum, New York, p 79
54. Dickstein P et al (1988) Adhesives conference, vol 3. Pergamon Press, London, p 1668
55. Dos Reis HLM, Vary A (1988) In: 1988 Fall Conference, vol 1. Soc Exp Mech, p 2649
56. Guyott CCH, Cawley P (1988) Proceedings of the 4th European conference on non-destructive testing, vol 3. Pergamon Press, London, p 1678
57. Mal AK et al (1988) New Directions in the Nondestruct Eval of Adv Mat, Mat Div Pub MD, vol 9. ASME, p 85
58. Pilarski A, Rose JL (1988) NDT Int 21:241
59. Pilarski A et al (1988) Proceedings of the 4th European conference on non-destructive testing, vol 2237. Pergamon Press, London, UK, p 4
60. Yuhus EE et al (1988) In: H. Ishida (ed) Interface in polymer, ceramic and metal matrix composites. Elsevier, New York, p 595
61. Dickstein P et al (1989) J Nondestruct Eval 8:27. doi:[10.1007/BF00566585](https://doi.org/10.1007/BF00566585)
62. Duke JC Jr et al (1989) NASA CR-4195 NASA
63. Rose JL et al (1989) 17th symposium on nondestructive evaluation, vol. 1. Southwest Research Institute, San Antonio, p 276
64. Rokhlin SI, Marom D (1990) J Acoust Soc Am 87:532. doi:[10.1121/1.2028004](https://doi.org/10.1121/1.2028004)
65. Visscher WM et al (1990) Rev Prog Quant Nondestruct Eval 10B:1289, Plenum
66. Jiao D, Rose JL (1991) J Adhes Sci Technol 5:631
67. Reighard MK et al (1991) Mater Eval 49:1506
68. Rose JL (1991) Adhesive bonding, vol 1. Plenum Publishing, Corp, New York, p 425
69. Crawley PC et al (1992) Rev Prog Quant Nondestruct Eval 12B:1531, Plenum
70. Pialucha TP, Cawley P (1992) PRI third international conference on structural adhesives in engineering III 21 Plastics and Rubber Institute, Bristol
71. Pialucha T, Cawley P (1992) Rev Prog Quant Nondestruct Eval 11B:1261, Plenum
72. Rokhlin SI et al (1993) Res Nondestruct Eval 5:95. doi:[10.1007/BF01606359](https://doi.org/10.1007/BF01606359)
73. Singher L et al (1994) J Acoust Soc Am 96:2497. doi:[10.1121/1.410123](https://doi.org/10.1121/1.410123)
74. Rose JL et al (1994) Rev Prog Quant Nondestruct Eval 14B:1417, Plenum
75. Singher L et al (1994) Rev Prog Quant Nondestruct Eval 14B:1481, Plenum
76. Zurn B, Mantell, SC (1999) In: 44th International SAMPE Symposium and Exhibition, 44, book 2:1246 SAMPE
77. Kwon O-Y, Lee S-H (1999) NDT E Int 32:153. doi:[10.1016/S0963-8695\(98\)00066-8](https://doi.org/10.1016/S0963-8695(98)00066-8)
78. Krautkramer J, Krautkramer H (1983) Ultrasonic testing of materials, 3rd edn. Springer-Verlag, New York
79. Hart-Smith LJ (1982) AFWAL-TR-82-4172 Air Force Wright Aeronautical Laboratories Technical Report
80. Hart-Smith LJ (1993) Adv mat: performance through technology insertion, vol 38. I. SAMPE, p 226
81. Hart-Smith LJ (1995) Materials challenge: diversification and the future, vol 40-II. SAMPE, Covina CA, p 1124
82. Hart-Smith LJ (1995) Materials challenge: diversification and the future, vol 40-II. SAMPE, Atlanta, p 1134
83. Hart-Smith LJ, Thrall EW (1985) Adhesive bonding of aluminum alloys. Marcel Dekker, Inc, p 323

84. Georgiou GA et al (1997) TWI J 6:630
85. Gol'den AD (1993) Soviet J Nondestruct Test (Defektoskopiya) 1:39
86. Guo N, Lim MK (1995) Rev Prog Quant Nondestruct Eval 15A:323, Plenum
87. Guy P et al (1990) J Phys 51:supplement C-2:1249
88. He F et al (1987) Rev Prog Quant Nondestruct Eval 7B, Plenum Publishing
89. Kundu T, Blodgett M (1994) Rev Prog Quant Nondestruct Eval 13B:1343, Plenum
90. Mal AK et al (1989) Int J Eng Sci 27:779. doi:[10.1016/0020-7225\(89\)90045-1](https://doi.org/10.1016/0020-7225(89)90045-1)
91. Mal AK et al (1990) J Eng Mat Tech 112:255
92. Rokhlin SI (1984) Analytical ultrasonics in materials research and testing, vol 1. NASA, Cleveland, OH, p 299
93. Rokhlin SI (1987) Materials analysis by ultrasonics: metals, ceramics, composites, vol 1. Noyes Publications, p 290
94. Rose JL, Diriti JJ (1992) Br J Nondestruct Test 34:591
95. Sun KJ, Johnston PH (1993) Rev Prog Quant Nondestruct Eval 13B:1507, Plenum
96. Teller CM, Diercks KJ (1987) Rev Prog Quant Nondestruct Eval 7B:935, Plenum
97. Vasudeva RY, Rao PG (1992) J Appl Phys 71:612. doi:[10.1063/1.350414](https://doi.org/10.1063/1.350414)
98. Xu P-C et al (1990) Int J Eng Sci 28:331. doi:[10.1016/0020-7225\(90\)90106-S](https://doi.org/10.1016/0020-7225(90)90106-S)
99. Bossi RH et al (2002) Mater Eval 60:1333
100. Frock BG et al (1997) UDR-TR-97-133 University of Dayton Research Institute
101. Crane RL (2001) Structural integrity of composite materials and structures: optimisation of micro-structural design, 23 May
102. Bossi RH et al Application No. 20030079552 Assigned to Boeing
103. Bossi RH et al (2004) SAMPE conference: M&P technology - 60 years of SAMPE progress, May 16–20
104. Primary Adhesively Bonded Structural Technology (PABST): Design Handbook for Adhesive Bonding (1979) AFFDL-TR-79-3129 Air Force Flight Dynamics Laboratory
105. Primary Adhesively Bonded Structure Technology (PABST): Tooling, Fabrication & QA Report (1979) AFFDL-TR-79-3154 Air Force Flight Dynamics Laboratory
106. Potter DL (1979) AFFDL-TR-79-3129 Air Force Flight Dynamics Laboratory Technical Report
107. Thrall EW Jr (1979) Structural Adhesives and Bonding. Technology Conferences Assoc., El Segundo, CA, p 293
108. Smith T (1984) SAMPE Q 15:6
109. Smith T (1983) 20/20 Vision in Materials for 2000 576 SAMPE, Covina CA
110. Smith T (1979) Rev Prog Quant Nondestruct Eval 1:275, Air Force Materials Laboratory
111. Smith T (1979) Structural Adhesives and Bonding. Technology Conferences Assoc., El Segundo, CA, p 190
112. Smith T, Lindberg G (1979) Surf Tech 9:1. doi:[10.1016/0376-4583\(79\)90080-3](https://doi.org/10.1016/0376-4583(79)90080-3)
113. Smith T (1977) AFML-TR-77-42 Air Force Materials Laboratory Technical Report
114. Smith T (1975) Mater Eval 33:101
115. Rimmel TP (1976) AFML-TR-76-118 Air Force Materials Laboratory
116. Rantz LE (1987) Adhaes Age 30:10
117. Cibula A et al (1986) Testing of metallic and inorganic coatings. American Society for Testing and Materials, Philadelphia, p 329
118. Garrett CE, Good EF (1978) Surface contamination: genesis, detection and control, vol 2. Plenum, New York, p 857
119. Hunter W et al (1970) Surf Sci 20:355. doi:[10.1016/0039-6028\(70\)90188-3](https://doi.org/10.1016/0039-6028(70)90188-3)
120. Kawai A et al (1994) J Ceram Soc Jpn 102:1102
121. Kim DH, Sutliff EF (1978) SAMPE Q 9:59
122. Kollek H, Brockmann W (1978) Surface contamination: genesis, detection and control, vol 2. Plenum, Washington, DC, p 713
123. Kuhn AT (1993) Met Finish 91:25
124. Smith T (1976) Surf Sci 56:212. doi:[10.1016/0039-6028\(76\)90448-9](https://doi.org/10.1016/0039-6028(76)90448-9)
125. White HW et al (1978) Rev Prog Quant Nondestruct Eval, vol 1. Air Force Materials Laboratory, p 186
126. Zurbrick JR (1977) Int Adv Nondestruct. Test. vol 1. Gordon & Breach, London, p 41
127. Kulkarni PG, Totlani MK (1993) Trans Met Finish Assoc India 2:37
128. Smith AC, Yang H (1989) Mater Eval 47:1396
129. Smith T (1975) SAMPE materials review, vol 75. SAMPE, Covina CA, p 349
130. Lipson AG et al (1990) Doklady Akademii Nauk SSSR 310:1398
131. Rider A, Vodicka R (2004) DSTO-RR-0282 Defence Sci. Tech. Org, Air Vehicles Div
132. Segal E, Kenig S (1989) Mater Eval 47:921
133. van Avery J (1996) Materials and process challenges: aging systems, affordability, alternative applications, vol 41-II. SAMPE, p 1203
134. Boerio FJ et al (1990) Surf Interface Anal 17:448. doi:[10.1002/sia.740170707](https://doi.org/10.1002/sia.740170707)
135. Boerio FJ et al (2006) J Adhes 82:19. doi:[10.1080/00218460500418516](https://doi.org/10.1080/00218460500418516)
136. Gent AN, Schultz J (1972) J Adhes 3:281. doi:[10.1080/00218467208072199](https://doi.org/10.1080/00218467208072199)
137. Andrews EH, Kinloch AJ (1973) Proc Royal Soc 332:385. doi:[10.1098/rspa.1973.0032](https://doi.org/10.1098/rspa.1973.0032)
138. Maugis D (1985) J Mater Sci 20:3041. doi:[10.1007/BF00545170](https://doi.org/10.1007/BF00545170)
139. van Oss CJ et al (1988) Chem Rev 88:927. doi:[10.1021/cr00088a006](https://doi.org/10.1021/cr00088a006)
140. Kaelble DH, Uy KC (1970) J Adhes 2:66. doi:[10.1080/0021846708544582](https://doi.org/10.1080/0021846708544582)
141. Fries JA (1982) Int J Adhes Adhesi 2:187. doi:[10.1016/0143-7496\(82\)90088-4](https://doi.org/10.1016/0143-7496(82)90088-4)
142. Satas D (ed) (1989) Handbook of pressure sensitive adhesives technology, 2nd edn. Van Nostrand, New York, p 89
143. Coughlin T (2001) Austin TX 30: 1 www.ntiac.com